UNDERSTANDING TWO-FLAVOR OSCILLATION PARAMETERS AND LIMITS

Revised March 2002 by D.E. Groom (LBNL).

As discussed in Boris Kayser's Review "Neutrino Mass, Mixing, and Flavor Change," there are several conditions under which the two-neutrino mixing approximation is valid. Many results have been published with this assumption, whether it is valid or not. In this context, and in the context of vacuum oscillations, the probability that a neutrino with original flavor ℓ, for example, oscillates into a flavor ℓ' over a distance L in vacuum is given by

$$\begin{aligned} P(\nu_\ell \to \nu_{\ell'}) &= \sin^2 2\theta \sin^2(\Delta m^2_{ij} L/4\hbar cE) \\ &= \sin^2 2\theta \sin^2(1.27 \Delta m^2_{ij}(\mathrm{eV}^2)\, L(\mathrm{km})/E(\mathrm{GeV})) \end{aligned} \tag{1}$$

where we assume that mass eigenstates i and j are involved. Although this equation is frequently quoted and is used in Monte Carlo calculations, the function is badly behaved for arguments larger than about one, where it oscillates more and more rapidly between $\sin^2 2\theta = P$ and $\sin^2 2\theta = 0$ as the argument increases. It is difficult to relate this function to the exclusion curves in the literature.

In a real experiment, E, and sometimes L, have some spread due to various effects, but in a subset of these experiments there is a well-defined $\langle L/E \rangle$ about which the events distribute. It is instructive to make a toy model in which $b \equiv 1.27 L/E$ has a Gaussian distribution with standard deviation σ_b about a central value b_0. The convolution of this Gaussian with P as given in Eq. (1) is analytic, with the result

$$\langle P \rangle = \tfrac{1}{2} \sin^2 2\theta [1 - \cos(2 b_0 \Delta m^2_{ij}) \exp(-2\sigma_b^2 (\Delta m^2_{ij})^2)] \ . \tag{2}$$

The value of $\langle P \rangle$ is set by the experiment. For example, if 230 interactions of the expected flavor are detected and none of the wrong flavor are seen, then $P = 0.010$ at the 90% CL (slightly subject to one's way of calculating the CL). Then with fixed $\langle P \rangle$ we can find $\sin^2 2\theta$ as a function of Δm^2_{ij}. This function is shown in Fig. 1(a) and (c) for particular parameter choices. The

resulting parameter exclusion region boundary has the following features:

(1) For large Δm^2_{ij} the fast oscillations are completely washed out by the resolution, and $\sin^2 2\theta = 2\langle P\rangle$ in this limit;

(2) the maximum excursion of the curve to the left is to $\sin^2 2\theta = \langle P\rangle$ if the resolution is very good, and somewhat smaller if it is not. This "bump" to the left occurs at $\Delta m^2_{ij} = \pi/2b_0$;

(3) For large $\sin^2 2\theta$, $\Delta m^2_{ij} \approx \sqrt{\langle P\rangle}/(b_0\sqrt{\sin^2 2\theta})$; and, consequently,
   (a) the nearly straight-line segment at the bottom is described by $\Delta m^2_{ij} \approx \langle P\rangle/b_0\sqrt{\sin^2 2\theta}$
   (b) the intercept at $\sin^2 2\theta = 1$ is at $\Delta m^2_{ij} = \sqrt{\langle P\rangle}/b_0 = \sqrt{\langle P\rangle}/1.27\langle L/E\rangle$.

The intercept for large Δm^2_{ij} is a measure of running time and backgrounds, while the intercept at $\sin^2 2\theta = 1$ also depends upon $\langle L/E\rangle$. The wiggles depend upon the experimental features such as the size of the source, the neutrino energy distribution, detector resolution (L and E), and analysis details. Aside from such details, the two intercepts completely describe the exclusion region: For large Δm^2_{ij}, $\sin^2 2\theta$ is constant and equal to $2\langle P\rangle$, and for large $\sin^2 2\theta$ the slope and intercept are known. For these reasons, it is (nearly) sufficient to summarize the results of an experiment by stating the two intercepts, as is done in our Listings in cases where two-neutrino analyses of this sort have been published.

While there is no reason for such a naïve 3-parameter function to describe all real experiments, the function actually does give a remarkably good description of *some* experimental results, underscoring the usefulness of the way we report results in the Listings. In example (a) in Fig. 1, the dotted curve shows the result obtained in an old Los Alamos appearance experiment (DURKIN 88). DURKIN 88 reports $\Delta m^2 = 0.11$ eV^2 for maximal mixing and $\sin^2 2\theta = 2 \times 0.070$ for large Δm^2. The solid curve is obtained using Eq. (2), with parameters $\langle P\rangle = 0.0065$, $\Delta m^2 = 0.095$ eV^2 at $\sin^2 2\theta = 1$, and $\sigma_b/b_0 = 0.23$.

If a positive effect is claimed, then the excluded region is replaced by an allowed band. However, in a real experiment

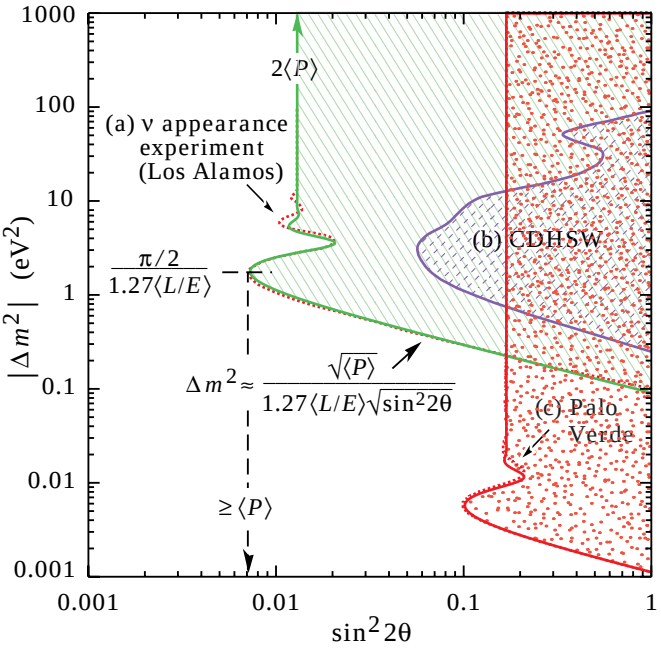

Figure 1: Neutrino oscillation parameter ranges excluded by three experiments. The dotted line in (a) is from an older Los Alamos appearance experiment (DURKIN 88), while the solid line is obtained from Eq. (2) using the parameters $\langle P\rangle = 0.0065$, $\Delta m^2 = 0.095$ eV^2 at $\sin^2 2\theta = 1$, and $\sigma_b/b_0 = 0.23$; (b) is a disappearance experiment with the flux obtained from the data in a long detector (DYDAK 84); and for (c) the Palo Verde reactor experiment result (BOEHM 01) is shown by the dotted line. In this experiment the flux at production is known. The solid line is calculated from Eq. (2) using $\langle P\rangle = 0.084$, $\Delta m^2 = 0.0011$ eV^2 at $\sin^2 2\theta = 1$, and $\sigma_b/b_0 = 0.3$. The experiments have been chosen for illustrative purposes, and none represents a current best limit. See full-color version on color pages at end of book.

there is usually other information, such as estimators of L and E for each event. The likelihood function is formed using this event-by-event information. The CL is not uniform along the allowed band, resulting in "islands" of high confidence.

In a "disappearance" experiment, one looks for the attenuation of the initial lepton eigenstate ν_ℓ beam in transit to a detector, where the ν_ℓ flux is measured. (We label such experiments as $\nu_\ell \not\to \nu_\ell$.) In the two-neutrino mixing approximation,

the probability that a lepton eigenstate remains unscathed from the production point to the detector is given by

$$P(\nu_\ell \to \nu_\ell) = 1 - P(\nu_\ell \to \nu_{\ell'}) \ , \tag{3}$$

where mixing occurs between the ν_ℓ and $\nu_{\ell'}$, with $P(\nu_\ell \to \nu_{\ell'})$ given by Eq. (1) or Eq. (2).

The disappearance of a small fraction of the "right-flavor" neutrinos in such an experiment can go unobserved because of statistical fluctuations—if 100 events are expected and 95 events are observed, nothing is proven.* For this reason, disappearance experiments usually cannot establish small-probability (small $\sin^2 2\theta$) mixing.

Disappearance experiments fall into several classes:

(1) Those in which attenuation or oscillation of the beam neutrino flux is measured in the apparatus itself (two detectors, or a "long" detector). Above some minimum Δm^2_{ij} the equilibrium is established upstream, and there is no change in intensity over the length of the apparatus. As a result, sensitivity is lost at high Δm^2_{ij}, as can be seen by the CDHSW curve, Fig. 1(b) (DYDAK 84). Such experiments have not been competitive for a long time. However, a new generation of long-baseline experiments will use this strategy to advantage.

(2) Accelerator and reactor experiments in which the beam neutrino flux is known, from theory or from other measurements. Although such experiments cannot establish very small $\sin^2 2\theta$ mixing, they can establish small limits on Δm^2_{ij} for large $\sin^2 2\theta$ because L/E can be very large. Results of the Palo Verde experiment (BOEHM 01) are shown by the dotted curve (c) in Fig. 1. The solid curve has been calculated via Eq. (2), with parameters $\langle P \rangle = 0.084$, $\Delta m^2 = 0.0011$ eV^2 at $\sin^2 2\theta = 1$ (very nearly the values reported in BOEHM 01), and $\sigma_b/b_0 = 0.3$.

(3) Atmospheric neutrino experiments, in which ν_e and ν_μ are detected over a large range of L (the diameter of the earth).

* In contrast, if 5 golden "wrong-flavor" events are seen among 100 "right-flavor" events, a great deal is learned.

This is a subset of (1) above, and the resulting curves, in this case showing a positive effect, are similar.

This discussion has so far been limited to "vacuum oscillations," where the mixing probability is described Eq. (1). In the solar neutrino case it is likely that interactions between the neutrinos and solar electrons affect the oscillation probability ("matter oscillations," the MSW effect). This effect is described in the Review "Neutrino Mass, Mixing, and Flavor Change," by Boris Kayser. In this situation the formalism discussed above is not applicable.

Eq. (1) depends on the mixing angle only through $\sin^2 2\theta$, giving the false impression that physically distinct possibilities map one-to-one onto the interval [0,1] in $\sin^2 2\theta$.† The relationship between mass eigenstates, *e.g.*, ν_1, ν_2, and weak eigenstates, *e.g.*, ν_e, ν_μ, is given by

$$\begin{pmatrix} |\nu_1\rangle \\ |\nu_2\rangle \end{pmatrix} = \begin{pmatrix} \cos\theta & -\sin\theta \\ \sin\theta & \cos\theta \end{pmatrix} \begin{pmatrix} |\nu_e\rangle \\ |\nu_\mu\rangle \end{pmatrix} \quad . \tag{4}$$

By convention, we can take ν_2 always heavier than ν_1, *i.e.*, $\Delta m^2_{21} = m^2_2 - m^2_1 > 0$, without a loss of generality. The $\theta \to 0$ limit is relevant when there is no mixing and ν_e is lighter, while $\theta \to \pi/2$ is needed to describe the possibility where ν_e is heavier with no mixing. Therefore, θ needs to be varied between 0 and $\pi/2$, which makes $\sin^2 2\theta$ fold at 1 back down to 0. In the case of oscillation in vacuum, θ and $\pi/2 - \theta$ happen to give identical oscillation probabilities, even though they are physically inequivalent. In this case, the use of $\sin^2 2\theta$ is misleading, but acceptable from practical point of view. In presence of matter effects, even the oscillation probabilities are different, and $\sin^2 2\theta$ is not an appropriate parameter in oscillation parameter plots. One common choice is $\tan^2\theta$, because it can cover the whole range of $0 \le \theta \le \pi/2$, while showing the same probabilities for $\theta \leftrightarrow \pi/2 - \theta$ in the absence of matter effects as a reflection symmetry around $\tan^2\theta = 1$ if plotted on log scale.‡

† For example, see G.L. Fogli, E. Lisi, and D. Montanino, Phys. Rev. **D54**, 2048 (1996), and A. de Gouvêa, A. Friedland, and H. Murayama, Phys. Lett. **B490**, 125 (2000)

‡ This discussion of the $\pi/4 \le \theta \le \pi/2$ region was contributed by H. Murayama.